Published in final edited form as:
Sci Transl Med. 2013 July 24; 5(195): 195ra97. doi:10.1126/scitranslmed.3006135.

CaMKII Is Essential for the Proasthmatic Effects of Oxidation

Philip N. Sanders[1], **Olha M. Koval**[1], **Omar A. Jaffer**[1], **Anand M. Prasad**[1], **Thomas R. Businga**[1], **Jason A. Scott**[1], **Patrick J. Hayden**[2], **Elizabeth D. Luczak**[1], **David D. Dickey**[1], **Chantal Allamargot**[3], **Alicia K. Olivier**[4], **David K. Meyerholz**[4], **Alfred J. Robison**[5], **Danny G. Winder**[6], **Timothy S. Blackwell**[7], **Ryszard Dworski**[7], **David Sammut**[8], **Brett A. Wagner**[9], **Garry R. Buettner**[9], **Robert M. Pope**[10], **Francis J. Miller Jr.**[1,11], **Megan E. Dibbern**[1], **Hans Michael Haitchi**[8], **Peter J. Mohler**[12], **Peter H. Howarth**[8], **Joseph Zabner**[1], **Joel N. Kline**[1], **Isabella M. Grumbach**[1,11,13,*], and **Mark E. Anderson**[1,11,14,*]

[1]Department of Internal Medicine, Carver College of Medicine, University of Iowa, Iowa City, IA 52242, USA

[2]MatTek Corporation, 200 Homer Avenue, Ashland, MA 01721, USA

[3]Central Microscopy Research Facilities, University of Iowa, Iowa City, IA 52242, USA

[4]Department of Pathology, Medical Laboratories, University of Iowa, Iowa City, IA 52242, USA

[5]Department of Physiology, Michigan State University, East Lansing, MI 48824, USA

[6]Department of Molecular Physiology and Biophysics, Vanderbilt University School of Medicine, Nashville, TN 37232, USA

[7]Department of Internal Medicine, Vanderbilt University School of Medicine, Nashville, TN 37232, USA

[8]Clinical and Experimental Sciences, Faculty of Medicine, University of Southampton and NIHR Respiratory Bioscience Research Unit, Southampton General Hospital, Southampton, Hants SO16 6YD, UK

[9]Free Radical and Radiation Biology Program, Department of Radiation Oncology, University of Iowa, Iowa City, IA 52242, USA

[*]Corresponding author: mark-e-anderson@uiowa.edu (M.E.A.); isabella-grumbach@uiowa.edu (I.M.G.).

Author contributions

M.E.A., I.M.G., and J.N.K. described the initial hypothesis. M.E.A., J.N.K., J.Z., P.J.M., I.M.G., R.M.P., F.J.M., and P.N.S. designed the experiments and M.E.A., I.M.G., and P.N.S. analyzed the data and wrote the paper. Most data in this paper were generated by P.N.S., with the exception of, immunofluorescence imaging of human and murine tissue (C.A., O.A.J., M.E.D., and P.N.S.), MUC5AC scoring (P.N.S. and O.A.J.), epithelial thickness measurements (P.N.S. and O.A.J.), CaMKII activity assays (A.M.P.), flexiVent assessment of AHR (T.R.B., O.A.J., and P.N.S.), BAL differential cell counts (O.A.J. and T.R.B.), EPR data (P.N.S., O.A.J., B.A.W., and G.R.B.), immunoblots (P.N.S., A.M.P., and O.A.J.), luciferase assays (P.N.S. and J.A.S.), human and murine epithelial cell work (P.N.S., O.A.J., and D.D.D.), Cl− channel current measurements (O.M.K.), mRNA analysis (O.A.J. and P.N.S.), MM-VV adenovirus production (P.N.S. and E.D.L.), baculoviral CaMKII production (E.D.L.), and mass spectrometry (R.M.P.). The tetO-GFP-AC3-I mice were generated by D.G.W. and A.J.R., and the HLL mice were generated by T.S.B. P.J.H., D.S., R.D., H.M.H., and P.H.H. provided the human lung tissue sections; D.K.M. and A.K.O. helped devise the mucus scoring system.

Competing interests

M.E.A., I.M.G., and J.N.K. are named inventors on a patent application from The University of Iowa claiming to treat asthma by CaMKII inhibition. Methods of Treating Pulmonary Diseases and Disorders by Modulating Calcium/Calmodulin Dependent Protein Kinase II Activity, Patent Number US 20110152172 A1. M.E.A. is a cofounder of Allosteros Therapeutics, a biotech aiming to develop enzyme inhibitor therapies. The remaining authors declare no competing interests.

[10]Proteomics Facility, University of Iowa, Iowa City, IA 52242, USA

[11]University of Iowa Cardiovascular Research Center, Iowa City, IA 52242, USA

[12]The Dorothy M. Davis Heart and Lung Research Institute, The Ohio State University Wexner Medical Center, Columbus, OH 43210, USA

[13]Iowa City VA Healthcare System, Iowa City, IA 52246, USA

[14]Department of Molecular Physiology and Biophysics, Carver College of Medicine, University of Iowa, Iowa City, IA 52242, USA

Abstract

Increased reactive oxygen species (ROS) contribute to asthma, but little is known about the molecular mechanisms connecting increased ROS with characteristic features of asthma. We show that enhanced oxidative activation of the Ca^{2+}/calmodulin-dependent protein kinase (ox-CaMKII) in bronchial epithelium positively correlates with asthma severity and that epithelial ox-CaMKII increases in response to inhaled allergens in patients. We used mouse models of allergic airway disease induced by ovalbumin (OVA) or Aspergillus fumigatus (Asp) and found that bronchial epithelial ox-CaMKII was required to increase a ROS- and picrotoxin-sensitive Cl^- current (I_{Cl}) and MUC5AC expression, upstream events in asthma progression. Allergen challenge increased epithelial ROS by activating NADPH oxidases. Mice lacking functional NADPH oxidases due to knockout of p47 and mice with epithelial-targeted transgenic expression of a CaMKII inhibitory peptide or wild-type mice treated with inhaled KN-93, an experimental small molecule CaMKII antagonist, were protected against increases in I_{Cl}, MUC5AC expression, and airway hyper-reactivity to inhaled methacholine. Our findings support the view that CaMKII is a ROS-responsive, pluripotent pro-asthmatic signal and provide proof-of-concept evidence that CaMKII is a therapeutic target in asthma.

Introduction

Asthma afflicts 8.5% of the U.S. population and is estimated to cause over 3000 deaths and cost over $56 billion annually in lost work and medical expenses (1). Adequate asthma control cannot be achieved with standard treatment approaches in a majority of patients (2), suggesting that improved understanding of disease mechanisms and identification of new therapies will be necessary to reduce the suffering and expenses associated with asthma. Asthma patients have increased reactive oxygen species (ROS) measured in exhaled gas (3) compared to healthy controls; ROS signaling is implicated in characteristic features of asthma, including goblet cell hyperplasia (4), airway inflammation (5), and airway hyper-reactivity (AHR) (6). Despite the clear connection between elevated pulmonary ROS and asthma, molecular mechanisms explaining ROS-triggered asthma progression and therapeutic approaches addressing the role of ROS in asthma are lacking. Ca^{2+}/calmodulin-dependent protein kinase (CaMKII) is a master regulatory molecule and an attractive candidate signal for promoting diseases where elevated ROS contributes to disease initiation or progression (7). Under resting conditions, CaMKII is held in an inactive state, but increased levels of calcified calmodulin (Ca2+/CaM) activate CaMKII by binding to the regulatory domain (8). Once activated, CaMKII can retain activity in the absence of

Ca^{2+}/CaM binding by oxidation at Met281/282 (9). CaMKII activity is enhanced by Met281/282 oxidation (ox-CaMKII) because these modifications prevent inhibitory re-occlusion of the catalytic domain by the autoinhibitory domain (8). Active CaMKII catalyzes the phosphorylation of proteins that increase inflammatory signaling (10), cell proliferation (11), and ion channel activity (12). Excessive ROS promotes diseases (7), but few examples are known in which molecular signals couple ROS to clearly defined downstream signaling pathways in specific cell types. We recently found that excessive levels of ox-CaMKII contribute to heart disease (9, 13, 14), suggesting that ox-CaMKII could participate in disease processes initiated or aggravated by increased ROS in non-cardiac tissues. We asked whether CaMKII could be an important, but previously unrecognized, pro-asthmatic signal and whether CaMKII inhibition could protect against asthma. Here we show that ox-CaMKII expression positively correlates with asthma severity and is increased by exposure to inhaled allergens in patients. We developed a genetic mouse model of bronchial epithelium–targeted CaMKII inhibition to provide experimental evidence validating a previously unrecognized pathway where CaMKII in bronchial epithelium is required for ROS-induced pro-asthmatic responses. We found that genetic and pharmacological CaMKII inhibition reduces the severity of core disease markers in ovalbumin (OVA)– and Aspergillus fumigatus (Asp)–treated mice, models of allergic airway disease (15, 16). Our findings point to CaMKII as a candidate target for asthma therapies.

Results

Bronchial ox-CaMKII is increased in asthma patients and OVA mice

Asthma patients have increased ROS in lung tissue and in their exhaled breath (3), which we hypothesized may favor increased levels of ox-CaMKII. We measured ox-CaMKII, using an antiserum raised against oxidized Met281/282 (9), in bronchial biopsy specimens from normal (n = 11) and severely asthmatic (n = 14) individuals with treatment-resistant disease (table S1). Although CaMKII expression was evident in bronchial epithelium and airway smooth muscle, ox- CaMKII was predominantly present in the bronchial epithelium (Fig. 1, A and B). Severe asthmatics showed a significant increase in ox-CaMKII [P = 0.009, n = 11 healthy, 14 severely asthmatic, Mann-Whitney (MaWh) used to determine significance; Fig. 1, A and C] without change in total CaMKII (tot-CaMKII) (Fig. 1, B and D). We next turned to the OVA model to investigate whether ox-CaMKII contributes to OVA-induced airway disease. The OVA model (see Materials and Methods for details) recapitulates key features of human asthma, including increased ROS, airway inflammation, goblet cell hyperplasia, mucus secretion, and AHR (15). Lungs from OVA mice showed significantly increased ox-CaMKII (P = 0.002, n = 6 per group, MaWh; Fig. 1, E and F) without increased tot-CaMKII (Fig. 1, E and G). Quantitative immunoblots on mouse lung homogenates showed that ox-CaMKII expression was significantly increased in OVA mice compared to saline-treated controls (P = 0.004, n = 8 per group, MaWh; Fig. 1, H and I). Epitope competition assays validated the specificity of our ox-CaMKII antisera in human and murine lung sections (fig. S1), and we detected increased ox-CaMKII in OVA compared to vehicle treated mouse lungs by mass spectrometry (fig. S2). The OVA model represents sub acute allergen exposure; thus, we next analyzed ox-CaMKII levels in bronchial biopsy sections from mild

asthmatics, naive to steroid treatment, before and after allergen challenge. Ox-CaMKII in the bronchial epithelium was significantly increased after allergen challenge in mild asthmatics, suggesting that ox-CaMKII levels correlated with sub acute allergen exposure in asthma patients (P = 0.023, n = 15 mild asthma before allergen challenge, n = 15 mild asthma after allergen challenge, Wilcoxon; Fig. 1, J and K). We saw no variation in tot-CaMKII levels in the epithelium or smooth muscle before or after allergen exposure (Fig. 1, L and M). We next compared epithelial CaMKII levels in healthy individuals, mild asthmatics before allergen challenge, and severe asthmatics, and found that ox-CaMKII levels increased significantly with increasing disease severity [P = 0.039, n = 17, 15, and 10 respectively, analysis of variance (ANOVA); fig. S3]. In contrast, tot-CaMKII levels did not vary between these groups. These data show that ox-CaMKII expression positively correlates with asthma severity and is increased in bronchial epithelium from asthmatic, allergen-challenged patients and in OVA mice compared to controls. We interpret these findings to support the view that bronchial ox-CaMKII is an indicator of asthma severity, and to suggest that ox-CaMKII may contribute to the pathophysiology of allergic asthma.

Ox-CaMKII is regulated in vivo in OVA mice

We measured ROS levels in the lungs of saline and OVA mice using dihydroethidium (DHE) staining and found a significant increase in ROS after OVA (P = 0.001, n = 8 saline, n = 9 wild-type OVA, ANOVA with Bonferonni's correction; Fig. 2, A and B), consistent with reports of elevated ROS in asthmatic patients (3) and in OVA mice (17). The p47phox protein is required for Nox1 and Nox2 ROS-generating activity (18), and we found that $p47^{-/-}$ OVA mice were protected from OVA triggered ROS generation, with significantly reduced levels of ROS in the bronchial epithelium compared to wild-type OVA (P = 0.002, n = 9 wild-type OVA, n = 9 $p47^{-/-}$ OVA, MaWh; Fig. 2, A and B). However, ROS levels in $p47^{-/-}$ OVA mice were not statistically different from those in wild-type saline-treated mice (P = 0.16, n = 8 wild-type saline, MaWh; Fig. 2, A and B). To further quantify oxidative stress in the airways, we measured the levels of ascorbate radical, a marker of oxidative stress (19), in whole-lung homogenates using electron paramagnetic spectroscopy, and found a significant increase in ascorbate radical levels in wild-type OVA mice compared to $p47^{-/-}$ OVA mice (P = 0.017, n = 9 wild-type OVA, n = 6 $p47^{-/-}$ OVA, MaWh; fig. S4,A and B). We next measured tot-CaMKII and ox-CaMKII in $p47^{-/-}$ and wild-type littermate controls. $p47^{-/-}$ mice showed significantly less ox- CaMKII compared to wild-type mice after OVA (P = 0.017, n = 8 per groups, MaWh; Fig. 2, C and D). Tracheal epithelial cells isolated from $p47^{-/-}$ mice showed reduced levels of ox-CaMKII after cytokine challenge compared to wild-type control cells (P = 0.05, n = 3, ANOVA with Bonferroni's correction; fig. S5, A and B). In contrast, the levels of tot-CaMKII were similar in both the saline-treated and OVA mice (Fig. 2E). Our data in $p47^{-/-}$ mice suggest that NADPH oxidases contribute to increased ROS and ox-CaMKII in OVA mice. Oxidative activation of CaMKII correlates with disease severity We next asked whether the reduced ROS in p47−/− OVA mice affected disease severity. The $p47^{-/-}$ OVA mice showed a significant reduction in goblet cell hyperplasia (Fig. 3A), bronchial epithelial thickness (P = 0.0001, n = 7 per group, MaWh; Fig. 3B), MUC5AC (mucin)–positive airway cells [P = 0.016, n = 10 per group, MaWh (Fig. 3C), and P = 0.0003, n = 10 per group (fig. S6A)], Muc5ac mRNA expression (P = 0.005, n = 10 per group, MaWh; Fig. 3D), airway eosinophilia (P = 0.036, n = 12, per

group, MaWh; Fig. 3E), and the eosinophil attractant chemokine Ccl-11 (P = 0.022, n = 6 per group, MaWh; Fig. 3F) compared to OVA wild-type mice. We interpret our data to show that NADPH oxidases are required for increasing ox-CaMKII (Fig. 2, C and D) and that inhibition of NADPH oxidases by p47 knockout reduces core disease outcomes in OVA mice. The improvement of these key OVA induced pathologies in $p47^{-/-}$ mice mirrors previously published data (20) and studies from our laboratory showing improvement in characteristic features of asthma with a clinically validated glucocorticoid therapy (fig. S7). Our findings suggest an important role for Nox-derived ROS in oxidative activation of CaMKII and potentially in the progression of key disease traits in OVA mice. Methionine sulfoxide reductase A (MsrA) is an antioxidant enzyme capable of reversing methionine oxidation (21). MsrA has been shown to reduce ox-CaMKII after angiotensin II or aldosterone challenge in heart (9, 14). $Msra^{-/-}$ OVA mice exhibited a significant increase in goblet cell hyperplasia (Fig. 3G), bronchial epithelial thickness (P = 0.0001, n = 7 per group, MaWh; Fig. 3H), MUC5AC-positive cells (P = 0.008, n = 9 per group, MaWh; Fig. 3I and fig. S6B), Muc5ac mRNA levels (P = 0.018, n = 8 per group, MaWh; Fig. 3J), airway eosinophilia (P = 0.013, n = 13 per group, MaWh; Fig. 3K), and mRNA expression of the eosinophil attractant chemokine Ccl-11 (P = 0.05, n = 6 per group, MaWh; Fig. 3l). Our data show that manipulation of genetic pathways for ROS generation affects the severity of disease characteristics (reduced in $p47^{-/-}$ and increased in $Msra^{-/-}$) and is potentially consistent with a role of oxidatively activated CaMKII in promoting asthma. Enhanced nuclear factor kB (NF-kB) activity is a consistent finding and central event in asthma progression (22). NF-kB activity is believed to be important for activating inflammatory signaling pathways in asthma (22) and increasing MUC5AC expression (23). Therefore, we next confirmed that NF-kB activity was increased in our OVA mice. We used NF-kB luciferase reporter mice (10, 24) interbred with $p47^{-/-}$ or $Msra^{-/-}$ mice. OVA mice expressing the NF-kB reporter had significant induction of NF-kB activity compared to saline-challenged NF-kB reporter mice (P = 0.01, n > 4 saline, n > 6 OVA, ANOVA with Bonferroni's correction; fig. S8, A and B). OVA NF-kB reporter mice lacking p47 had a significant reduction in NF-kB activity (P = 0.023, n = 10 per group, MaWh; fig. S8A) compared to OVA wild type littermate control mice, whereas OVA mice lacking Msra exhibited a significant increase in NF-kB activity (P = 0.029, n = 6 per group, MaWh; fig. S8B) compared to OVA wild-type littermate control mice. Together, these data show that NF-kB activity responds to genetic manipulation of ROS pathways and correlates with ox-CaMKII expression and disease severity.

Ox-CaMKII increases ICl in airway epithelium

Chloride currents (I_{Cl}) are present on the bronchial epithelia (25), and increased activity of I_{Cl} channels, in particular g-aminobutyric acid type A receptor ($GABA_AR$), is strongly associated with goblet cell hyperplasia in OVA mice and in human asthmatic airways (25). CaMKII (26) and ROS (27) can also increase I_{Cl}, suggesting the potential interdependence of ROS and CaMKII in regulating airway epithelial I_{Cl} activity. We measured I_{Cl} activity in tracheal epithelial cells isolated from OVA- and saline- treated mice using whole cell–mode voltage (patch) clamp. I_{Cl} was significantly increased in OVA compared to saline-treated tracheal epithelial cells (P = 0.001, n = 8 saline, n = 10 OVA, ANOVA with Bonferroni's correction; Fig. 4, A to C). The $GABA_AR$ antagonist picrotoxin (PTXN) significantly

reduced peak I_{Cl} recorded from OVA mice toward values recorded in saline controls (P = 0.002, n = 10 OVA, n = 11 OVA + PTXN, MaWh; Fig. 4, A to C), consistent with previous findings showing that OVA treatment increases a PTXN sensitive I_{Cl} (25). Addition of the CaMKII inhibitor KN-93 (28) significantly reduced peak I_{Cl} recorded from OVA mice (P = 0.015, n = 10OVA, n = 4 OVA + KN-93, MaWh; Fig. 4C) but did not further reduce I_{Cl} after PTXN (Fig. 4, A to C), suggesting that the CaMKII-sensitive (27) and PTXN sensitive (25) components of I_{Cl} were equivalent. In addition, we found decreased levels of MUC5AC after interleukin-13 (IL-13) challenge in isolated human tracheal epithelial cells after treatment with PTXN and also in cells expressing the CaMKII inhibitor CaMKIIN or an oxidant resistant CaMKII (MM-VV) (fig. S9, A and B), suggesting that CaMKII and I_{Cl} contribute to mucus production in OVA mice. We next asked whether OVA-induced I_{Cl} was decreased in $p47^{-/-}$ mice, and whether ox-CaMKII was required for OVA- and ROS-mediated increases in I_{Cl}. We measured I_{Cl} in tracheal epithelial cells from saline- and OVA-treated wildtype and $p47^{-/-}$ mice and tracheal epithelial cells from saline-treated mice infected with lentivirus to overexpress wild-type CaMKII or an oxidant-resistant CaMKII mutant (MM-VV) (9). We found that peak I_{Cl} was equivalent in cells isolated from saline-treated wild-type and $p47^{-/-}$ mice, but reduced in OVA $p47^{-/-}$ mice compared to OVA wild-type mice (P = 0.001, n = 10 OVA, n = 6 $p47^{-/-}$ OVA, MaWh; Fig. 4, D to F), suggesting that ROS derived from NADPH oxidases enhanced I_{Cl} in OVA mice. We added H_2O_2 (200 mM) to tracheal epithelial cells over expressing wild-type CaMKII, MM-VV CaMKII, or CaMKIIN (29), a CaMKII inhibitory peptide. We found a significant increase in I_{Cl} in cells over expressing wild-type CaMKII compared to mock-infected cells (P = 0.05, n = 6 mock, n = 5 wildtype CaMKII, MaWh; Fig. 4I), but cells over expressing the oxidant resistant MM-VV CaMKII mutant (Fig. 4, G to I) or CaMKIIN (fig. S10, A to C) were unable to increase I_{Cl}. Over expression of wild-type or MM-VV CaMKII in the absence of H_2O_2 did not affect baseline I_{Cl} (fig. S10D). The relative lentiviral-driven CaMKII expression levels were similar (fig. S11), indicating that differential responses to H_2O_2 were not due to different levels of wild-type or MM-VV CaMKII expression. We interpret these findings to show that ox-CaMKII promotes I_{Cl} in OVA- and H_2O_2-treated pulmonary epithelium, actions that are anticipated to increase airway mucus (25).

Epithelial-targeted CaMKII inhibition reduces disease severity

To test whether increased bronchial epithelial CaMKII activity was important for in vivo disease markers in OVA mice, we designed mice with tetracycline-induced (tetO) transgenic expression of a CaMKII inhibitory peptide (AC3-I) (30) fused with enhanced green fluorescent protein (tetO-eGFP-AC3-I). Details of the development of this epithelial targeted CaMKII inhibition model (Epi-AC3-I) can be found in fig. S12 and in Supplementary Methods. Wild-type OVA mice showed a significant increase in AHR compared to saline controls (P = 0.005, n = 4 saline, n = 9 OVA, MaWh; Fig. 5A). The OVA epi-AC3-I mice showed reduced AHR (in response to methacholine; P = 0.0002, n = 9 wild-type OVA, n = 8 Epi-AC3-I, MaWh; Fig. 5A), goblet cell hyperplasia (Fig. 5B), bronchial epithelial thickening (P = 0.008, n = 7 per group, MaWh; Fig. 5C), airway MUC5AC (P = 0.019, n = 7 per group, MaWh; Fig. 5, B and D), Muc5ac mRNA (P = 0.038, n = 10 per group, MaWh; Fig. 5E), and airway mucus levels (P = 0.035, n = 10 per group, MaWh; fig. S6C) compared to OVA wild-type mice. There was a significant increase in ICl in cells from OVA wild-type

mice compared to wild-type saline (P = 0.01, n = 7 per group, ANOVA with Bonferroni's correction; Fig. 5, F to H). However, epi-AC3-I mice were resistant to OVA-triggered increases in I_{Cl} compared to tracheal epithelial cells isolated from OVA wild-type mice (P = 0.017, n = 7 per group, MaWh; Fig. 5H). Epi-AC3-I mice also exhibited decreased *Ccl-11* mRNA expression (P = 0.004, n = 7 per group, MaWh; Fig. 5I), eosinophilic airway infiltration (P = 0.013, n = 12 wild-type OVA, n = 11 Epi-AC3-I OVA, MaWh; Fig. 5J), and CaMKII activity (P = 0.015, n = 5 wild-type OVA, n = 4 Epi-AC3-I OVA, MaWh; Fig. 5K). We found that bronchial epithelial CaMKII inhibition was also protective in the Asp model of allergic airway disease. In this model, epi-AC3-I mice exhibited a significant reduction in AHR, airway MUC5AC, epithelial thickness, MUC5AC-positive cells, Muc5ac mRNA levels, *Ccl*-11 mRNA levels, and airway eosinophils (fig. S13). The airway epithelium expresses cytokines such as granulocyte macrophage colony-stimulating factor (GM-CSF), IL-5, and IL-1b that can enhance airway smooth muscle contraction and contribute to AHR (31–34). Lipopolysaccharide challenge in isolated tracheal epithelial cells, infected with adenovirus expressing CaMKIIN or an empty vector, showed that CaMKII inhibition reduced GM-CSF, IL-1β, and IL-5 mRNA expression at 12 and 24 hours (fig. S14). These data obtained from mice with genetic, epithelial-targeted CaMKII inhibition and from murine cultured tracheal epithelial cells support the concept that epithelial CaMKII inhibition is protective against allergic airway disease. KN-93 reduces disease severity and suppresses NF-kB activity We next performed a proof-of-concept study to test the potential therapeutic value of CaMKII inhibition in asthma by inhalation of an experimental small-molecule CaMKII inhibitor (KN-93) (28). The OVA mice treated with inhaled KN-93 showed a significant decrease in AHR (P = 0.013, n = 8 wild-type OVA, n = 7 OVA + KN-93, MaWh; Fig. 6A), goblet cell hyperplasia (P = 0.011, n = 7 wild-type OVA, n = 6 OVA + KN-93, MaWh; Fig. 6, B and C, and fig. S6D), epithelial thickness (P = 0.004, n = 7 wild-type OVA, n = 6 OVA + KN-93, MaWh; Fig. 6D), and Muc5ac mRNA levels (P = 0.029, n = 7 wild type OVA, n = 10 OVA + KN-93, MaWh; Fig. 6E). KN-93 also inhibited I_{Cl} in tracheal epithelial cells from OVA mice (P = 0.008, n = 10 wild-type OVA, n = 4 OVA + KN-93, MaWh; Fig. 6, F to H). These results suggest that inhaled CaMKII inhibitor drugs may be a useful therapeutic approach in allergic asthma. Increased NF-kB activation in the bronchial epithelium is sufficient to induce AHR in OVA mice (33), and the expression of cytokines able to modulate smooth muscle activity, such as GM-CSF (33). We previously showed that CaMKII inhibition is able to reduce the expression of GM-CSF in isolated epithelial cells (fig. S14); therefore, we next asked whether CaMKII inhibition could also reduce NF-kB activity. OVA mice had significant induction of NF-kB activity compared to saline-challenged NF-kB reporter mice (P = 0.05, n = 4 saline, n = 7 OVA, ANOVA with Bonferroni's correction; fig. S8C). KN-93 inhalation significantly reduced NF-kB activity (P = 0.037, n = 7 per group, MaWh; fig. S8C) in OVA mice. Furthermore, KN-93 inhalation reduced Ccl-11 expression (P = 0.006, n = 8 wild-type OVA, n = 10 OVA + KN-93, MaWh; Fig. 6I), airway eosinophilia (P = 0.03, n > 8 per group, MaWh; Fig. 6J), and CaMKII activity in whole-lung homogenates (P = 0.035, n = 3 wild-type OVA, n = 5 KN-93 OVA, MaWh; Fig. 6K) from OVA mice. These new data suggest that CaMKII inhibition reduces AHR, at least in part, as a consequence of diminished NF-kB activity.

Discussion

A now extensive body of evidence shows that excessive CaMKII activation promotes cardiovascular disease and that CaMKII inhibition improves pathological responses to ROS (7). On the basis of the emergent success of CaMKII inhibition in experimental models of heart disease, we reasoned that CaMKII inhibition may also be a feasible approach to treating asthma. Here, we provide evidence that ox-CaMKII positively regulates the activity of GABAA receptors and MUC5AC expression, established epithelial pro-asthmatic mechanisms (25). An intriguing feature of CaMKII is that it couples to many different downstream targets; thus, CaMKII inhibition may lead to benefit in asthma by actions at multiple pathways contributing to maladaptive phenotypes. CaMKII appears to orchestrate diverse asthma mechanisms in bronchial epithelium, a cell type accessible by inhaled drugs, and believed to be a key mediator of asthma (35). CaMKII inhibition and treatment with dexamethasone show similar therapeutic efficacy against disease defining markers in the OVA mice, suggesting that CaMKII inhibition may benefit a large number of steroid-unresponsive patients (2) and potentially avoid untoward side effects of chronic steroid use (36Because CaMKII inhibition also reduced NF-kB activity and the pro-inflammatory cytokine Ccl-11 (eotaxin-1), it is possible that inhaled CaMKII inhibitor drugs may be able to prevent inflammatory responses to pro-asthmatic stimuli by actions on the bronchial epithelium. The airway epithelium is believed to be an active participant in numerous remodeling and inflammatory events contributing to the progression of asthma (35). Our data provide new mechanistic understanding for the role of epithelium in pathological responses to ROS and may present a new target for therapeutic intervention. As our data places CaMKII downstream to ROS signaling in the epithelium, there may be “off target” effects of CaMKII inhibition on systems requiring ROS signaling to fight bacterial, viral, or fungal pathogens (37). Recent work has shown that IL-13, a cytokine implicated in asthma progression by $GABA_A$ receptor activation and MUC5AC expression (25), initiates a ROS burst that is required for MUC5AC production in cultured epithelial cells (38). Our data show that CaMKII is an essential component of the epithelial ROS-sensing machinery in OVA mice and suggest that ox-CaMKII may participate in epithelial responses to asthma in patients.

The OVA and Asp mice represent models of allergic airway disease, so it is unclear whether our results in these mice will be relevant to patients with non allergic asthma. Additionally, there are differences in murine airway structure and response to both OVA and Asp challenge, which means that translation into human studies requires further work. Furthermore, the number of human samples in our study does not allow us to make definitive conclusions about the presence of ox-CaMKII in various asthma subtypes (39). However, ox-CaMKII expression was sub acutely increased by allergens in patients with mild asthma and basal ox-CaMKII expression positively correlated with asthma severity, suggesting that ox-CaMKII is a marker of asthma severity.

It will be important and interesting to learn if increased ox-CaMKII is a general feature of asthma and if CaMKII inhibition is a viable approach to treating or preventing asthma exacerbations induced by multiple stimuli. Our new data are aligned with previous observations (5) showing that the activity of NADPH oxidases is an “upstream” ROS

generating mechanism that responds to proasthmatic allergens. However, we must also acknowledge the potential contribution of Duox 1 and 2, which are also found in human airway epithelium (40), to increased epithelial ROS. Our findings are consistent with the view that allergen evoked NADPH oxidases couple to disease-defining events in asthma through ox-CaMKII. We developed a mouse model with epithelial CaMKII inhibition to localize the pro-asthmatic effects of CaMKII to bronchial epithelium, but our findings do not exclude the possibility that CaMKII activity may also promote asthma by actions in other cell types, including airway smooth muscle (41) and macrophages (42). We investigated the contribution of airway smooth muscle to the OVA model used in our study, and found that CaMKII may play a role in modulating smooth muscle function through the release of cytokines known to effect smooth muscle constriction, such as GM-CSF, IL-5, and IL-1β (32–34). We interpret these data in combination with the finding that epithelial-delimited CaMKII inhibition was sufficient to prevent core asthma responses to support the view that bronchial epithelium provides an essential contribution in sub acute OVA and Asp models of allergic airway disease.

Our studies provide evidence for a previously unrecognized pro-asthmatic pathway where CaMKII is oxidatively activated by NADPH oxidases and where ox-CaMKII promotes I_{Cl}, goblet cell hyperplasia, activation of an inflammatory gene program transcription factor, expression of inflammatory cytokines, eosinophil invasion, and AHR. In particular, we show that NF-kB activation is positively regulated by ROS in our OVA model. NF-kB is a redox-responsive transcription factor, and ROS can either potentiate (43) or inhibit (44) its activation, depending on the inflammatory milieu. Although our findings are discrepant with one chronic granulomatous disease study (45), they agree with another study from the same group (46). Because NF-kB activation responses to injury are dependent on stimulus, timing, and cell type (10), it seems likely that variability of the NF-kB response is sensitive to differences in experimental models and protocols. Our study suggests that asthma is a disease in which excessive ox-CaMKII may contribute to important, disease-defining characteristics, in part by promoting the activity of NF-kB. Our findings are consistent with another recent study showing that the NADPH oxidase antagonist apocynin significantly attenuated OVA-induced AHR and inflammation (47). Current asthma therapies lack a target to mediate ROS signaling pathways, which significantly contribute to asthma severity (4–6). Here, we provide a new and potentially drugable target that is able to link upstream ROS signaling with downstream cellular outcomes relevant to the pathology of asthma.

Materials and design

Study design

To comply with the University's animal ethics policies, experimental design was such that the fewest number of animals were used to provide the required data. This was typically achieved by using <10 animals. Our OVA and Asp groups of $n > 6$ animals allowed us to perform sufficiently powered statistical analysis. Predefined endpoints were selected as key pathologies associated with asthma. Our study aimed to determine whether ox-CaMKII expression is increased in asthma and if ox-CaMKII contributes to asthma manifestations in two established mouse models of allergic airway disease. Oxidized CaMKII levels were

assessed via immunofluorescence in human and mouse tissue sections; goblet cell metaplasia and cytokine expression were quantified after CaMKII inhibition in mouse tissue and human epithelial cells. Chloride current activity was measured via patch clamp in murine epithelial cells, and AHR was determined in response to methacholine in mice, in response to CaMKII inhibition, using the Scireq flexiVent. Mice were assigned randomly to each treatment group after genotyping. Mucus scoring and measurement of epithelial thickness were performed by investigators blinded to treatment and genotype.

Animals

All animal care and housing requirements of the National Institutes of Health (NIH) Committee on Care and Use of Laboratory Animals were followed. All protocols were reviewed and approved by the University of Iowa Animal Care and Use Committee. $p47^{-/-}$ (48), C57Bl/6, B6D2, and CCSP-rtTa (49) mice were obtained from The Jackson Laboratory. $p47^{-/-}$ mice were bred into a B6D2 background (>8 generations). Mice lacking the protein MsrA [$Msra^{-/-}$ (21)] were supplied by the NIH. Details regarding the generation and characterization of tetO-GFP-AC3-I mice can be found in the Supplementary Materials.

Human lung tissue

Human lung tissues were obtained from bronchoscopy or organs donated for research with informed consent following approved protocols (NHLBI grant 1 R43 HL088807-01 to P.J.H., National Disease Research Interchange, Philadelphia, PA, Vanderbilt University Committee for the Protection of Human Subjects, Southampton and South West Hampshire Local Research Ethics Committees). Details of collection and fixation can be found in the Supplementary Materials.

OVA and Asp sensitization and challenge

Six- to eight-week-oldmale and female mice were sensitized by intraperitoneal injection of 10 μg of OVA (Sigma) mixed with 1 mg of alum (or saline alone, for control mice) at days 0 and 7. Mice were subsequently challenged with inhaled OVA (1% solution in 0.9% saline, 40-min challenge) or saline on days 15, 16, and 17 as previously described (15). Airway reactivity to methacholine was assessed 24 hours after the final exposure to OVA (day 18). Asp sensitization was performed as previously described (16) with the following modifications.

Mice were sensitized via intraperitoneal and subcutaneous injections with 20 μg of Asp crude extract (Greer Laboratories) dissolved in 0.2 ml of incomplete Freund adjuvant (Sigma-Aldrich). After four intranasal instillations of 10 μg of Asp at days 14, 21, 28, and 32, AHR in response to methacholine was measured on day 33.

Assessment of AHR

AHR in response to methacholine was measured on a flexiVent small animal ventilator (Scireq) using a single compartment model, giving the dynamic resistance of the respiratory system (R), as described previously (15). A full description of the protocol can be found in the Supplementary Materials.

Bronchoalveolar lavage

After the assessment of AHR, mice were euthanized. The trachea was cannulated and phosphate-buffered saline/1% bovine serum albumin washings were collected (BAL) for total and differential counts of lavage cells.

Intranasal administration of KN-93

Intranasal administration of KN-93 (Axxora) was performed as previously described (50) with modifications. Thirty minutes before inhalation of OVA on days 15, 16, and 17, B6D2 or HLL mice were anesthetized with isoflurane (5%); 20 μl of 100 μM KN-93 or deionized H2O was delivered into the nares as themice awoke. After administration, mice were monitored to ensure no solution was expelled, and their recovery, before returning to the cage.

Lung histology

Murine lungs were fixed with 4% paraformaldehyde and then processed by paraffin-embedding. Five-micron tissue sections were cut and stained with MUC5AC (Abcam) to score mucin distribution. MUC5AC-stained sections were scored using a ranking system (51) with modifications, as described. Mucus distribution (intensity of stain): 0, none; 1, <33%; 2, 34 to 66%; 3, 67 to 100% of positively stained epithelium per airway; further details on the methodology can be found in the Supplementary Materials. The thickness of the epithelial layer was measured in airways less than 500μm in diameter. Five separate measurements of five individual airways per sample were made in a blinded manner at ×400 magnification. Images were taken on an Olympus BX-61 light microscope at ×400 and ×1000.

Immunofluorescence

Human lung tissue (donor details in table S1) or lung sections from mice were probed for a-SMA (Santa Cruz Biotechnology) and oxidized or total CaMKII. Immune sera developed against total (52) and oxidized (9, 52) (Epitomics) CaMKII were used to visualize CaMKII. Alexa Fluor secondary antibodies (Invitrogen) were used to visualize staining, and TOPRO-3 was used to stain nuclei (Invitrogen). Sections were mounted with VectaShield mounting medium (VectaShield). Images were taken with a Zeiss 510 confocal microscope at ×400 or ×630 magnification. Intensity of oxidized or total CaMKII staining was determined using image acquisition and analysis software (ImageJ, NIH) and presented as mean fluorescence intensity per square micrometer. All images were taken at the same time and using the same imaging settings.

Immunoblots

Homogenate of flash-frozen lungs was prepared in radio immunoprecipitation assay buffer (52). Twenty micrograms of soluble proteins was separated by SDS–polyacrylamide gel electrophoresis under non-denaturing conditions. Total actin was used to confirm loading (Santa Cruz Biotechnology).

Quantitative real-time polymerase chain reaction

Total RNA was isolated using the Qiagen RNeasy column-based kits. Complementary DNA was prepared using the SuperScript III reverse transcription system (Invitrogen) with random nanomer primers. Expression of mRNA was quantified with the iQ LightCycler (Bio-Rad) and SYBR Green dye system, normalized to acidic ribosomal phosphoprotein (Arp) mRNA. Primer sequences can be found in the Supplementary Materials.

CaMKII activity assays

CaMKII activity was measured in whole-lung homogenates as a function of [^{32}P]adenosine triphosphate incorporation into a synthetic substrate (syntide-2, Sigma-Aldrich) at 30°C, as previously described (9).

ROS detection

ROS levels were assessed with DHE (5 μM; Invitrogen) in snap-frozen 10-μm sections of whole lung, as described previously (53). Sections were imaged with the Bio-Rad 1024 confocal microscope, and analyzed with ImageJ. Values were obtained from the epithelial layer of three airways per sections, measuring less than 500 μm in length, at ×200 magnification. All images were taken at the same time and using the same imaging settings. Data are presented as mean fluorescence intensity per square micrometer.

Epithelial cell culture

Primary murine tracheal epithelial cells were isolated as previously described (54). Cells were either used immediately after isolation and removal of adherent cells, to assess Cl^- currents in OVA- and saline challenged mice, or plated onto collagen (BD Biosciences)–coated coverslips and maintained in MTEC Plus culture medium as described previously (54). After 24 hours, cells were infected with lentivirus containing wild-type CaMKIId, empty vector, or an oxidant-resistant CaMKII mutant with a methionine-methionine to valine-valine mutation at M281/282 (MM-VV) (9). Virus was incubated for 24 hours before patching.

Cl^- current (I_{Cl})

Ionic membrane currents were measured with an Axon 200B patchclamp amplifier using a Digidata 1320A acquisition board driven by pClamp 8.0 software (Axon Instruments). All experiments were conducted at room temperature. Detailed methods can be found in the Supplementary Materials.

Statistical analysis

Data are shown as means ± SE unless stated otherwise. Quantification of MUC5AC or Alcian blue/periodic acid–Schiff staining is presented as median ± range. Groups were compared using ANOVA and post hoc comparisons tested using Bonferroni's correction or two-tailed nonparametric Mann-Whitney U tests, as appropriate. Wilcoxon signed rank tests were used to compare paired biopsy samples from mild asthmatics before and after allergen challenge. The GraphPad Prism statistical software program was used for the analyses. P <

0.05 was regarded as statistically significant, with * representing significance versus saline or vehicle control.

Supplementary Material

Refer to Web version on PubMed Central for supplementary material.

Acknowledgments

Special thanks to R. Askeland, Department of Pathology, The University of Iowa, for characterization of human tissue. We are grateful to P. Snyder and M. Welsh (Department of Internal Medicine, The University of Iowa) and D. Spitz (Program in Free Radical and Radiation Biology, The University of Iowa) for constructive criticism and helpful discussions. Funding: This work was funded by a grant from the Sandler Program for Asthma Research and the American Asthma Foundation, grants from the NIH (K23 HL080030-02, M01 RR-00095), and enabled by the Medical Research Council (MRC, UK) (programme grant and Wessex severe asthma cohort). P.H.H.'s research is enabled by the MRC (UK) (programme grant and Wessex severe asthma cohort) and H.M.H. is funded by an MRC Clinician Scientist Fellowship (G0802804). Mass spectrometry analysis was performed in the Roy J. Carver Charitable Trust–supported CCOM Proteomics Facility at the University of Iowa.

References and notes

1. Barnett SB, Nurmagambetov TA. Costs of asthma in the United States: 2002–2007. J Allergy Clin Immunol. 2011; 127:145–152. [PubMed: 21211649]
2. Kerstjens HA, Engel M, Dahl R, Paggiaro P, Beck E, Vandewalker M, Sigmund R, Seibold W, Moroni-Zentgraf P, Bateman ED. Tiotropium in asthma poorly controlled with standard combination therapy. N Engl J Med. 2012; 367:1198–1207. [PubMed: 22938706]
3. Jarjour NN, Calhoun WJ. Enhanced production of oxygen radicals in asthma. J Lab Clin Med. 1994; 123:131–136. [PubMed: 8288953]
4. Casalino-Matsuda SM, Monzón ME, Forteza RM. Epidermal growth factor receptor activation by epidermal growth factor mediates oxidant-induced goblet cell metaplasia in human airway epithelium. Am J Respir Cell Mol Biol. 2006; 34:581–591. [PubMed: 16424381]
5. Abdala-Valencia H, Earwood J, Bansal S, Jansen M, Babcock G, Garvy B, Wills-Karp M, Cook-Mills JM. Nonhematopoietic NADPH oxidase regulation of lung eosinophilia and airway hyperresponsiveness in experimentally induced asthma. Am J Physiol Lung Cell Mol Physiol. 2007; 292:L1111–L1125. [PubMed: 17293377]
6. Hulsmann AR, Raatgeep HR, den Hollander JC, Stijnen T, Saxena PR, Kerrebijn KF, de Jongste JC. Oxidative epithelial damage produces hyperresponsiveness of human peripheral airways. Am J Respir Crit Care Med. 1994; 149:519–525. [PubMed: 8306055]
7. Erickson JR, He J, Grumbach IM, Anderson ME. CaMKII in the cardiovascular system: Sensing redox states. Physiol Rev. 2011; 91:889–915. [PubMed: 21742790]
8. Griffith LC. Regulation of calcium/calmodulin-dependent protein kinase II activation by intra-molecular and intermolecular interactions. J Neurosci. 2004; 24:8394–8398. [PubMed: 15456810]
9. Erickson JR, Joiner ML, Guan X, Kutschke W, Yang J, Oddis CV, Bartlett RK, Lowe JS, O'Donnell SE, Aykin-Burns N, Zimmerman MC, Zimmerman K, Ham AJ, Weiss RM, Spitz DR, Shea MA, Colbran RJ, Mohler PJ, Anderson ME. A dynamic pathway for calcium-independent activation of CaMKII by methionine oxidation. Cell. 2008; 133:462–474. [PubMed: 18455987]
10. Singh MV, Kapoun A, Higgins L, Kutschke W, Thurman JM, Zhang R, Singh M, Yang J, Guan X, Lowe JS, Weiss RM, Zimmermann K, Yull FE, Blackwell TS, Mohler PJ, Anderson ME. Ca2+/calmodulin-dependent kinase II triggers cell membrane injury by inducing complement factor B gene expression in the mouse heart. J Clin Invest. 2009; 119:986–996. [PubMed: 19273909]
11. Li W, Li H, Sanders PN, Mohler PJ, Backs J, Olson EN, Anderson ME, Grumbach IM. The multifunctional Ca2+/calmodulin-dependent kinase II d (CaMKIId) controls neointima formation after carotid ligation and vascular smooth muscle cell proliferation through cell cycle regulation by p21. J Biol Chem. 2011; 286:7990–7999. [PubMed: 21193397]

12. Dzhura I, Wu Y, Colbran RJ, Balser JR, Anderson ME. Calmodulin kinase determines calcium-dependent facilitation of L-type calcium channels. Nat Cell Biol. 2000; 2:173–177. [PubMed: 10707089]

13. Swaminathan PD, Purohit A, Soni S, Voigt N, Singh MV, Glukhov AV, Gao Z, He BJ, Luczak ED, Joiner ML, Kutschke W, Yang J, Donahue JK, Weiss RM, Grumbach IM, Ogawa M, Chen PS, Efimov I, Dobrev D, Mohler PJ, Hund TJ, Anderson ME. Oxidized CaMKII causes cardiac sinus node dysfunction in mice. J Clin Invest. 2011; 121:3277–3288. [PubMed: 21785215]

14. He BJ, Joiner ML, Singh MV, Luczak ED, Swaminathan PD, Koval OM, Kutschke W, Allamargot C, Yang J, Guan X, Zimmerman K, Grumbach IM, Weiss RM, Spitz DR, Sigmund CD, Blankesteijn WM, Heymans S, Mohler PJ, Anderson ME. Oxidation of CaMKII determines the cardiotoxic effects of aldosterone. Nat Med. 2011; 17:1610–1618. [PubMed: 22081025]

15. Munroe ME, Businga TR, Kline JN, Bishop GA. Anti-inflammatory effects of the neurotransmitter agonist Honokiol in a mouse model of allergic asthma. J Immunol. 2010; 185:5586–5597. [PubMed: 20889543]

16. Moreira AP, Cavassani KA, Ismailoglu UB, Hullinger R, Dunleavy MP, Knight DA, Kunkel SL, Uematsu S, Akira S, Hogaboam CM. The protective role of TLR6 in a mouse model of asthma is mediated by IL-23 and IL-17A. J Clin Invest. 2011; 121:4420–4432. [PubMed: 22005301]

17. Park CS, Kim TB, Lee KY, Moon KA, Bae YJ, Jang MK, Cho YS, Moon HB. Increased oxidative stress in the airway and development of allergic inflammation in a mouse model of asthma. Ann Allergy Asthma Immunol. 2009; 103:238–247. [PubMed: 19788022]

18. Clark RA. Activation of the neutrophil respiratory burst oxidase. J Infect Dis. 1999; 179(Suppl 2):S309–S317. [PubMed: 10081501]

19. Buettner GR, Jurkiewicz BA. Ascorbate free radical as a marker of oxidative stress: An EPR study. Free Radic Biol Med. 1993; 14:49–55. [PubMed: 8384150]

20. Ikeda RK, Nayar J, Cho JY, Miller M, Rodriguez M, Raz E, Broide DH. Resolution of airway inflammation following ovalbumin inhalation: Comparison of ISS DNA and corticosteroids. Am J Respir Cell Mol Biol. 2003; 28:655–663. [PubMed: 12760963]

21. Moskovitz J, Bar-Noy S, Williams WM, Requena J, Berlett BS, Stadtman ER. Methionine sulfoxide reductase (MsrA) is a regulator of antioxidant defense and lifespan in mammals. Proc Natl Acad Sci USA. 2001; 98:12920–12925. [PubMed: 11606777]

22. Hart LA, Krishnan VL, Adcock IM, Barnes PJ, Chung KF. Activation and localization of transcription factor, nuclear factor-kB, in asthma. Am J Respir Crit Care Med. 1998; 158:1585–1592. [PubMed: 9817712]

23. Fujisawa T, Velichko S, Thai P, Hung LY, Huang F, Wu R. Regulation of airway MUC5AC expression by IL-1b and IL-17A; the NF-kB paradigm. J Immunol. 2009; 183:6236–6243. [PubMed: 19841186]

24. Blackwell TS, Yull FE, Chen CL, Venkatakrishnan A, Blackwell TR, Hicks DJ, Lancaster LH, Christman JW, Kerr LD. Multiorgan nuclear factor kappa B activation in a transgenic mouse model of systemic inflammation. Am J Respir Crit Care Med. 2000; 162:1095–1101. [PubMed: 10988136]

25. Xiang YY, Wang S, Liu M, Hirota JA, Li J, Ju W, Fan Y, Kelly MM, Ye B, Orser B, O'Byrne PM, Inman MD, Yang X, Lu WY. A GABAergic system in airway epithelium is essential for mucus overproduction in asthma. Nat Med. 2007; 13:862–867. [PubMed: 17589520]

26. Wagner JA, Cozens AL, Schulman H, Gruenert DC, Stryer L, Gardner P. Activation of chloride channels in normal and cystic fibrosis airway epithelial cells by multifunctional calcium/calmodulin-dependent protein kinase. Nature. 1991; 349:793–796. [PubMed: 1705665]

27. Jeulin C, Guadagnini R, Marano F. Oxidant stress stimulates Ca2+-activated chloride channels in the apical activated membrane of cultured nonciliated human nasal epithelial cells. Am J Physiol Lung Cell Mol Physiol. 2005; 289:L636–L646. [PubMed: 16148052]

28. Sumi M, Kiuchi K, Ishikawa T, Ishii A, Hagiwara M, Nagatsu T, Hidaka H. The newly synthesized selective Ca2+/calmodulin dependent protein kinase II inhibitor KN-93 reduces dopamine contents in PC12h cells. Biochem Biophys Res Commun. 1991; 181:968–975. [PubMed: 1662507]

29. Chang BH, Mukherji S, Soderling TR. Characterization of a calmodulin kinase II inhibitor protein in brain. Proc Natl Acad Sci USA. 1998; 95:10890–10895. [PubMed: 9724800]
30. Zhang R, Khoo MS, Wu Y, Yang Y, Grueter CE, Ni G, Price EE Jr, Thiel W, Guatimosim S, Song LS, Madu EC, Shah AN, Vishnivetskaya TA, Atkinson JB, Gurevich VV, Salama G, Lederer WJ, Colbran RJ, Anderson ME. Calmodulin kinase II inhibition protects against structural heart disease. Nat Med. 2005; 11:409–417. [PubMed: 15793582]
31. Spina D. Epithelium smooth muscle regulation and interactions. Am J Respir Crit Care Med. 1998; 158:S141–S145. [PubMed: 9817737]
32. Whelan R, Kim C, Chen M, Leiter J, Grunstein MM, Hakonarson H. Role and regulation of interleukin-1 molecules in pro-asthmatic sensitised airway smooth muscle. Eur Respir J. 2004; 24:559–567. [PubMed: 15459133]
33. Pantano C, Ather JL, Alcorn JF, Poynter ME, Brown AL, Guala AS, Beuschel SL, Allen GB, Whittaker LA, Bevelander M, Irvin CG, Janssen-Heininger YM. Nuclear factor-kB activation in airway epithelium induces inflammation and hyperresponsiveness. Am J Respir Crit Care Med. 2008; 177:959–969. [PubMed: 18263801]
34. Hakonarson H, Maskeri N, Carter C, Grunstein MM. Regulation of TH1- and TH2-type cytokine expression and action in atopic asthmatic sensitized airway smooth muscle. J Clin Invest. 1999; 103:1077–1087. [PubMed: 10194481]
35. Holgate ST, Lackie PM, Davies DE, Roche WR, Walls AF. The bronchial epithelium as a key regulator of airway inflammation and remodelling in asthma. Clin Exp Allergy. 1999; 29(Suppl 2): 90–95. [PubMed: 10421830]
36. Kuna P. Long-term effects of steroid therapy. Wiad Lek. 1998; 51(Suppl 1):12–18. [PubMed: 9610231]
37. Gao XP, Standiford TJ, Rahman A, Newstead M, Holland SM, Dinauer MC, Liu QH, Malik AB. Role of NADPH oxidase in the mechanism of lung neutrophil sequestration and microvessel injury induced by Gram-negative sepsis: Studies in p47phox$^{-/-}$ and gp91phox$^{-/-}$ mice. J Immunol. 2002; 168:3974–3982. [PubMed: 11937554]
38. Yadav UC, Aguilera-Aguirre L, Ramana KV, Boldogh I, Srivastava SK. Aldose reductase inhibition prevents metaplasia of airway epithelial cells. PLoS One. 2010; 5:e14440. [PubMed: 21203431]
39. Kim HY, Dekruyff RH, Umetsu DT. The many paths to asthma: Phenotype shaped by innate and adaptive immunity. Nat Immunol. 2010; 11:577–584. [PubMed: 20562844]
40. Geiszt M, Witta J, Baffi J, Lekstrom K, Leto TL. Dual oxidases represent novel hydrogen peroxide sources supporting mucosal surface host defense. FASEB J. 2003; 17:1502–1504. [PubMed: 12824283]
41. Luo SF, Chang CC, Lee IT, Lee CW, Lin WN, Lin CC, Yang CM. Activation of ROS/NF-kB and Ca2+/CaM kinase II are necessary for VCAM-1 induction in IL-1b-treated human tracheal smooth muscle cells. Toxicol Appl Pharmacol. 2009; 237:8–21. [PubMed: 19281832]
42. Liu X, Yao M, Li N, Wang C, Zheng Y, Cao X. CaMKII promotes TLR-triggered proinflammatory cytokine and type I interferon production by directly binding and activating TAK1 and IRF3 in macrophages. Blood. 2008; 112:4961–4970. [PubMed: 18818394]
43. Asehnoune K, Strassheim D, Mitra S, Kim JY, Abraham E. Involvement of reactive oxygen species in Toll-like receptor 4-dependent activation of NF-kB. J Immunol. 2004; 172:2522–2529. [PubMed: 14764725]
44. Reynaert NL, van der Vliet A, Guala AS, McGovern T, Hristova M, Pantano C, Heintz NH, Heim J, Ho YS, Matthews DE, Wouters EF, Janssen-Heininger YM. Dynamic redox control of NF-kB through glutaredoxin-regulated S-glutathionylation of inhibitory kB kinase b. Proc Natl Acad Sci USA. 2006; 103:13086–13091. [PubMed: 16916935]
45. Segal BH, Han W, Bushey JJ, Joo M, Bhatti Z, Feminella J, Dennis CG, Vethanayagam RR, Yull FE, Capitano M, Wallace PK, Minderman H, Christman JW, Sporn MB, Chan J, Vinh DC, Holland SM, Romani LR, Gaffen SL, Freeman ML, Blackwell TS. NADPH oxidase limits innate immune responses in the lungs in mice. PLoS One. 2010; 5:e9631. [PubMed: 20300512]

46. Koay MA, Christman JW, Segal BH, Venkatakrishnan A, Blackwell TR, Holland SM, Blackwell TS. Impaired pulmonary NF-kB activation in response to lipopolysaccharide in NADPH oxidase-deficient mice. Infect Immun. 2001; 69:5991–5996. [PubMed: 11553535]
47. Kim SY, Moon KA, Jo HY, Jeong S, Seon SH, Jung E, Cho YS, Chun E, Lee KY. Antiinflammatory effects of apocynin, an inhibitor of NADPH oxidase, in airway inflammation. Immunol Cell Biol. 2012; 90:441–448. [PubMed: 21709687]
48. Jackson SH, Gallin JI, Holland SM. The p47phox mouse knock-out model of chronic granulomatous disease. J Exp Med. 1995; 182:751–758. [PubMed: 7650482]
49. Tichelaar JW, Lu W, Whitsett JA. Conditional expression of fibroblast growth factor-7 in the developing and mature lung. J Biol Chem. 2000; 275:11858–11864. [PubMed: 10766812]
50. Novakovic ZM, Leinung MC, Lee DW, Grasso P. Intranasal administration of mouse [D-Leu-4]OB3, a synthetic peptide amide with leptin-like activity, enhances total uptake and bioavailability in Swiss Webster mice when compared to intraperitoneal, subcutaneous, and intramuscular delivery systems. Regul Pept. 2009; 154:107–111. [PubMed: 19344673]
51. Livraghi A, Grubb BR, Hudson EJ, Wilkinson KJ, Sheehan JK, Mall MA, O'Neal WK, Boucher RC, Randell SH. Airway and lung pathology due to mucosal surface dehydration in b-epithelial Na + channel-overexpressing mice: Role of TNF-a and IL-4Ra signaling, influence of neonatal development, and limited efficacy of glucocorticoid treatment. J Immunol. 2009; 182:4357–4367. [PubMed: 19299736]
52. Li H, Li W, Gupta AK, Mohler PJ, Anderson ME, Grumbach IM. Calmodulin kinase II is required for angiotensin II-mediated vascular smooth muscle hypertrophy. Am J Physiol Heart Circ Physiol. 2010; 298:H688–H698. [PubMed: 20023119]
53. Grobe AC, Wells SM, Benavidez E, Oishi P, Azakie A, Fineman JR, Black SM. Increased oxidative stress in lambs with increased pulmonary blood flow and pulmonary hypertension: Role of NADPH oxidase and endothelial NO synthase. Am J Physiol Lung Cell Mol Physiol. 2006; 290:L1069–L1077. [PubMed: 16684951]
54. You Y, Richer EJ, Huang T, Brody SL. Growth and differentiation of mouse tracheal epithelial cells: Selection of a proliferative population. Am J Physiol Lung Cell Mol Physiol. 2002; 283:L1315–L1321. [PubMed: 12388377]
55. Wiśniewski JR, Zougman A, Nagaraj N, Mann M. Universal sample preparation method for proteome analysis. Nat Methods. 2009; 6:359–362. [PubMed: 19377485]
56. Singer M, Lefort J, Vargaftig BB. Granulocyte depletion and dexamethasone differentially modulate airways hyperreactivity, inflammation, mucus accumulation, and secretion induced by rmIL-13 or antigen. Am J Respir Cell Mol Biol. 2002; 26:74–84. [PubMed: 11751206]
57. Roh GS, Shin Y, Seo SW, Yoon BR, Yeo S, Park SJ, Cho JW, Kwack K. Proteome analysis of differential protein expression in allergen-induced asthmatic mice lung after dexamethasone treatment. Proteomics. 2004; 4:3318–3327. [PubMed: 15378748]
58. Ling H, Zhang T, Pereira L, Means CK, Cheng H, Gu Y, Dalton ND, Peterson KL, Chen J, Bers D, Brown JH. Requirement for Ca2+/calmodulin–dependent kinase II in the transition from pressure overload–induced cardiac hypertrophy to heart failure in mice. J Clin Invest. 2009; 119:1230–1240. [PubMed: 19381018]
59. Anderson RD, Haskell RE, Xia H, Roessler BJ, Davidson BL. A simple method for the rapid generation of recombinant adenovirus vectors. Gene Ther. 2000; 7:1034–1038. [PubMed: 10871752]
60. Karp PH, Moninger TO, Weber SP, Nesselhauf TS, Launspach JL, Zabner J, Welsh MJ. An in vitro model of differentiated human airway epithelia. Methods for establishing primary cultures. Methods Mol Biol. 2002; 188:115–137. [PubMed: 11987537]
61. Vermeer PD, Harson R, Einwalter LA, Moninger T, Zabner J. Interleukin-9 induces goblet cell hyperplasia during repair of human airway epithelia. Am J Respir Cell Mol Biol. 2003; 28:286–295. [PubMed: 12594054]
62. Miller FJ Jr, Chu X, Stanic B, Tian X, Sharma RV, Davisson RL, Lamb FS. A differential role for endocytosis in receptor-mediated activation of Nox1. Antioxid Redox Signal. 2010; 12:583–593. [PubMed: 19737091]

63. Woo HJ, Bae CH, Song SY, Kim YW, Lee HM, Kim YD. Expression of glutaredoxin-1 in nasal polyps and airway epithelial cells. Am J Rhinol Allergy. 2009; 23:288–293. [PubMed: 19490803]
64. Singh MV, Swaminathan PD, Luczak ED, Kutschke W, Weiss RM, Anderson ME. MyD88 mediated inflammatory signaling leads to CaMKII oxidation, cardiac hypertrophy and death after myocardial infarction. J Mol Cell Cardiol. 2012; 52:1135–1144. [PubMed: 22326848]
65. Wagner BA, Venkataraman S, Buettner GR. The rate of oxygen utilization by cells. Free Radic Biol Med. 2011; 51:700–712. [PubMed: 21664270]
66. Dworski R, Simon HU, Hoskins A, Yousefi S. Eosinophil and neutrophil extracellular DNA traps in human allergic asthmatic airways. J Allergy Clin Immunol. 2011; 127:1260–1266. [PubMed: 21315435]
67. Djukanović R, Wilson JW, Lai CK, Holgate ST, Howarth PH. The safety aspects of fiberoptic bronchoscopy, bronchoalveolar lavage, and endobronchial biopsy in asthma. Am Rev Respir Dis. 1991; 143:772–777. [PubMed: 2008989]
68. Cliff WH, Frizzell RA. Separate Cl− conductances activated by cAMP and Ca^{2+} in Cl^{-} secreting epithelial cells. Proc Natl Acad Sci USA. 1990; 87:4956–4960. [PubMed: 2164213]
69. British Thoracic Society Scottish Intercollegiate Guidelines Network. British Guideline on the Management of Asthma. Thorax. 2008; 63(Suppl 4):iv1–121. [PubMed: 18463203]

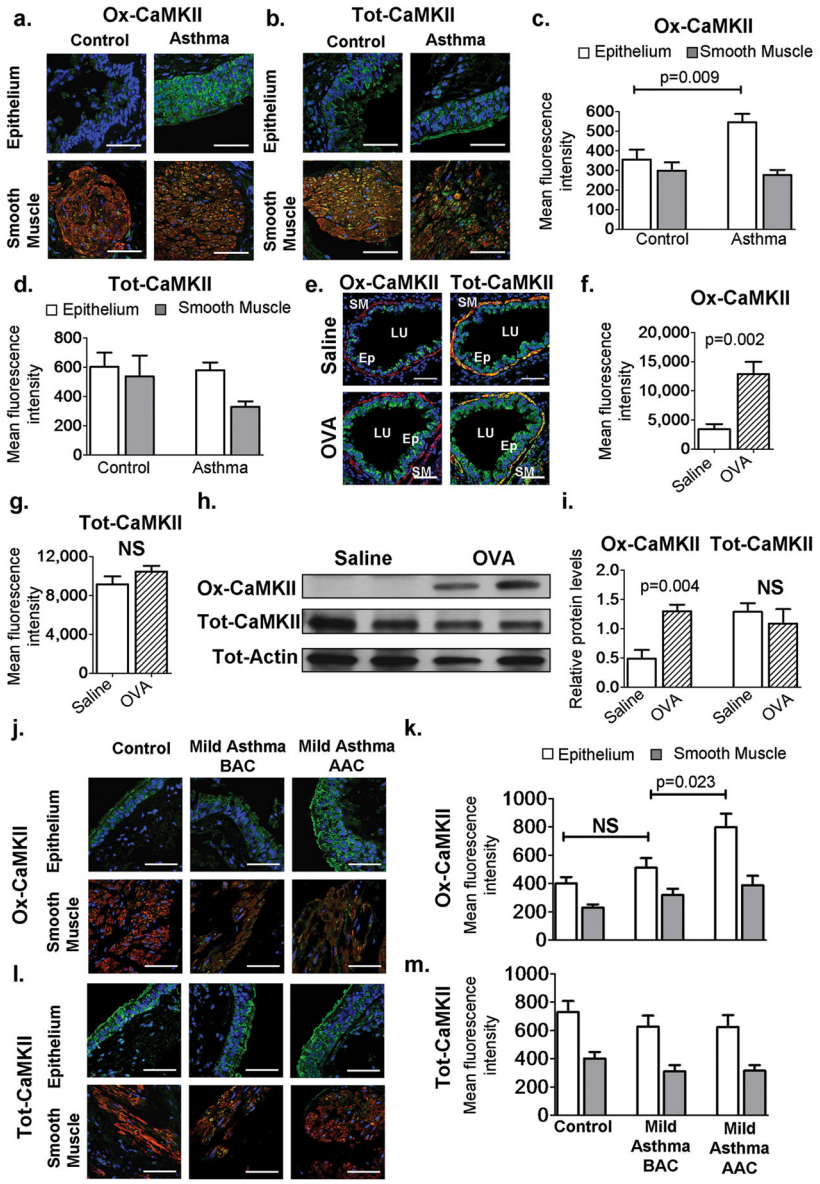

Fig. 1. Increased ox-CaMKII in asthmatic airway epithelium

(A and B) Localization of total and oxidized CaMKII in human airways (×400). Blue represents stained nuclei, green represents total (Tot) or ox-CaMKII, red represents α – smooth muscle actin (α-SMA), and yellow shows colocalization of CaMKII and α-SMA staining. (C and D) Mean fluorescence intensity of ox-CaMKII or tot-CaMKII staining in sections of human tissue per square micrometer (n = 14 asthma, n = 11 healthy), (E) Localization of ox-CaMKII or tot-CaMKII in murine airways (×400). In the panels, smooth muscle (SM), airway lumen (LU), and bronchial epithelium (Ep) are identified. (F and G) Mean fluorescence intensity per square micrometer of ox-CaMKII or tot-CaMKII staining in sequential sections of murine tissue (n = 6). (H) Representative ox-CaMKII and tot-CaMKII immunoblot images from murine whole-lung homogenates. (I). Quantification of immunoblots (n = 8 per group). Blots were stripped and re-probed for tot- CaMKII and tot-

actin. (J and K) Ox-CaMKII staining and quantification in the epithelium and smooth muscle of control patients (n = 9) and patients with mild asthma before allergen challenge (BAC; n = 15) and after allergen challenge (AAC; n = 15). (L and M) Staining and quantification of tot- CaMKII in the epithelium and smooth muscle of control patients (n = 9) and patients with mild asthma before allergen challenge (n = 15) and after allergen challenge (n = 15). NS, not significant. Scale bars, 50 μm. Mann- Whitney was used for comparisons between control and asthmatic patients, and saline and OVA mice. Wilcoxon signed rank was used for comparison of mild asthmatics before and after allergen challenge.

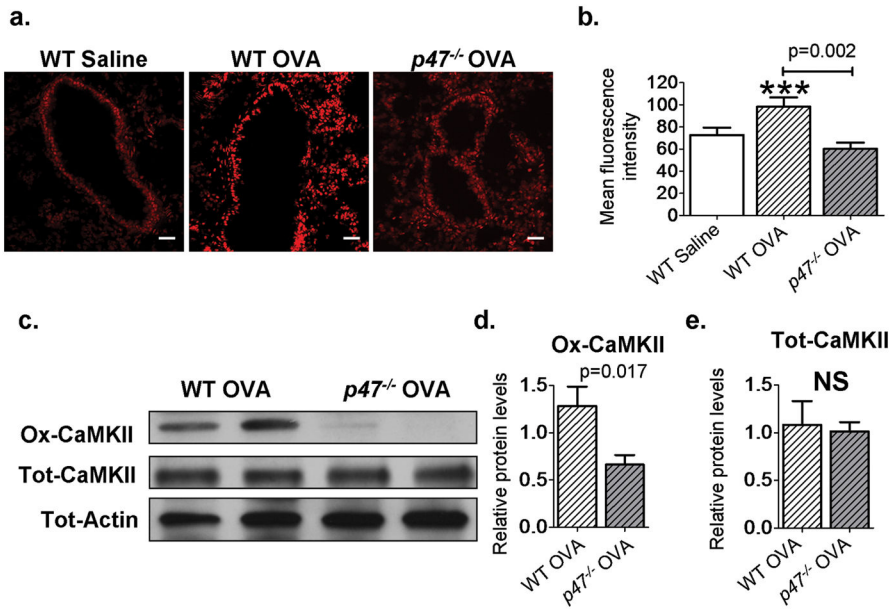

Fig. 2. Increased ROS in OVA mice leads to an up-regulation of ox-CaMKII

(A) DHE staining showing levels of ROS (×200). (B) Quantification of DHE staining in mouse lung sections; data show mean fluorescence intensity per square micrometer in the epithelium. Saline, n = 8; wild-type (WT) OVA, n = 9; $p47^{-/-}$ OVA, n = 9. (C) Immunoblot analysis of ox-CaMKII and tot-CaMKII in whole-lung homogenates from OVA WT and $p47^{-/-}$ mice. Immunoblots for WT saline, WT OVA, and $p47^{-/-}$ OVA are from the same gel as in Fig. 1H. (D and E) Quantification of immunoblot density of OVA WT (n = 8) and OVA $p47^{-/-}$ (n = 8). ***$P < 0.001$, versus saline control. Blots were stripped and re-probed for tot-CaMKII and tot-actin. Scale bars, 50 μm. ANOVA with Bonferroni's correction was used to compare saline to OVA; Mann-Whitney was used for OVA-to-OVA comparison.

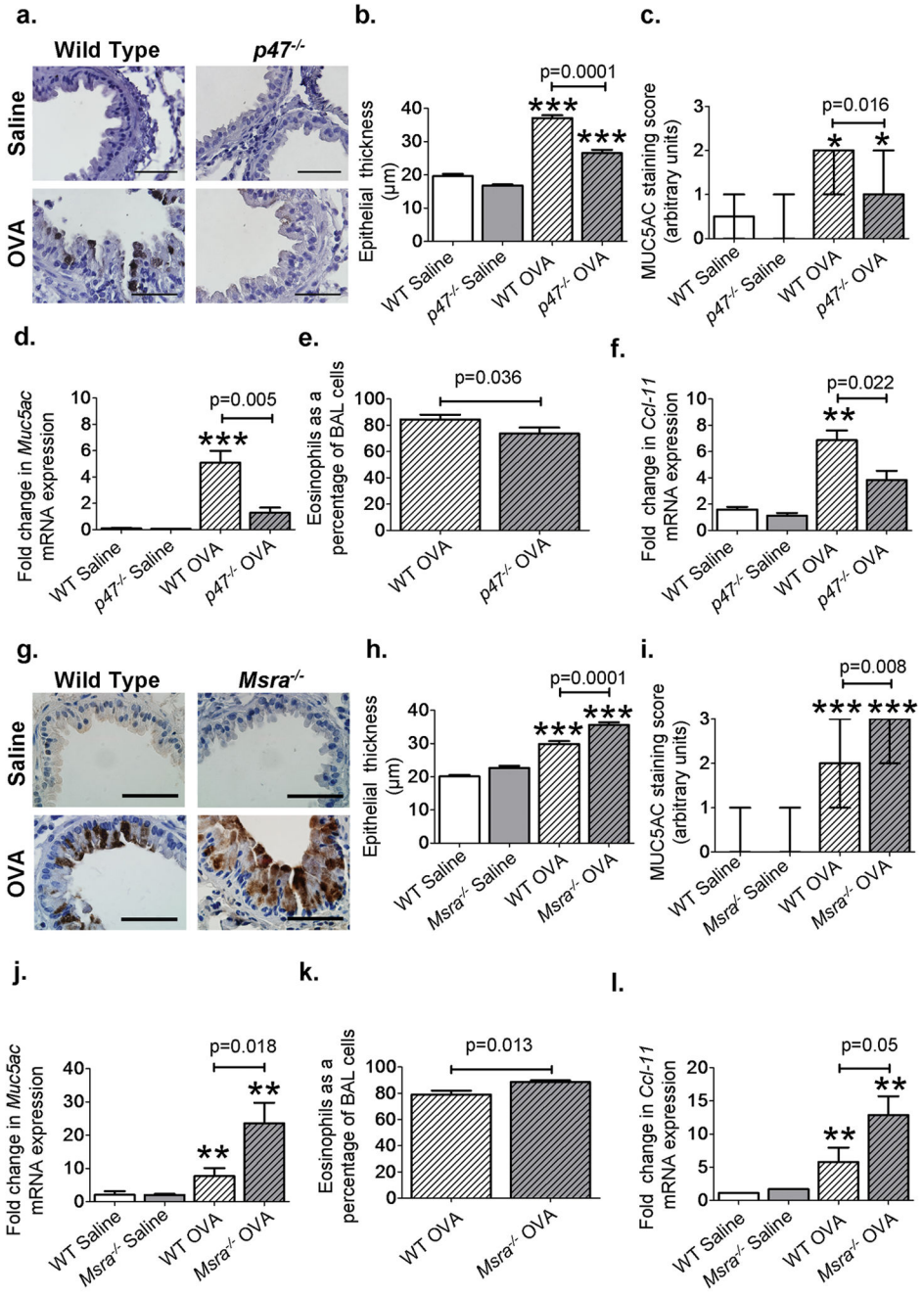

Fig. 3. ROS pathways determine disease severity

(A) Representative images of MUC5AC-stained (brown) sections highlighting goblet cell hyperplasia in saline and OVA WT and p47$^{-/-}$ airways (×1000). (B) Epithelial thickness in saline (n = 4 per group), OVAp47$^{-/-}$, and OVA WT airways (n = 7 per group). (C and D) Scoring of MUC5AC-positive cells in the airways and Muc5ac mRNA expression in whole-lung homogenates, saline controls (n = 4), p47−/− OVA mice (n = 10), and OVA WT mice (n = 10). (E and F) Eosinophil chemo-attractant *Ccl-11* mRNA levels (saline groups n > 4, OVA groups n = 6) and bronchoalveolar lavage (BAL) eosinophils (n = 12) as a percentage

of total cells in OVA p47$^{-/-}$ mice compared to OVA WT mice. (G) Representative images of MUC5AC staining in saline and OVAWT and MsrA$^{-/-}$ airways (×1000). (H) Epithelial thickness in murine airways (saline n > 4, OVA n = 7 per group). (I and J) MUC5AC-positive cells (saline n > 4, OVA n=9 per group) in the airways and *Muc5ac* mRNA expression (saline n=4, OVA n = 8 per group) in whole-lung homogenates. (K and L) BAL eosinophils (n = 13 per group) and *Ccl-11* mRNA levels in whole-lung homogenates (saline n=4, OVA n=6 per group). *P < 0.05, **P < 0.01, ***P < 0.001, versus saline control. Scale bars, 50 μm. ANOVA with Bonferroni's correction was used to compare saline to OVA; Mann-Whitney was used for OVA-to-OVA comparison.

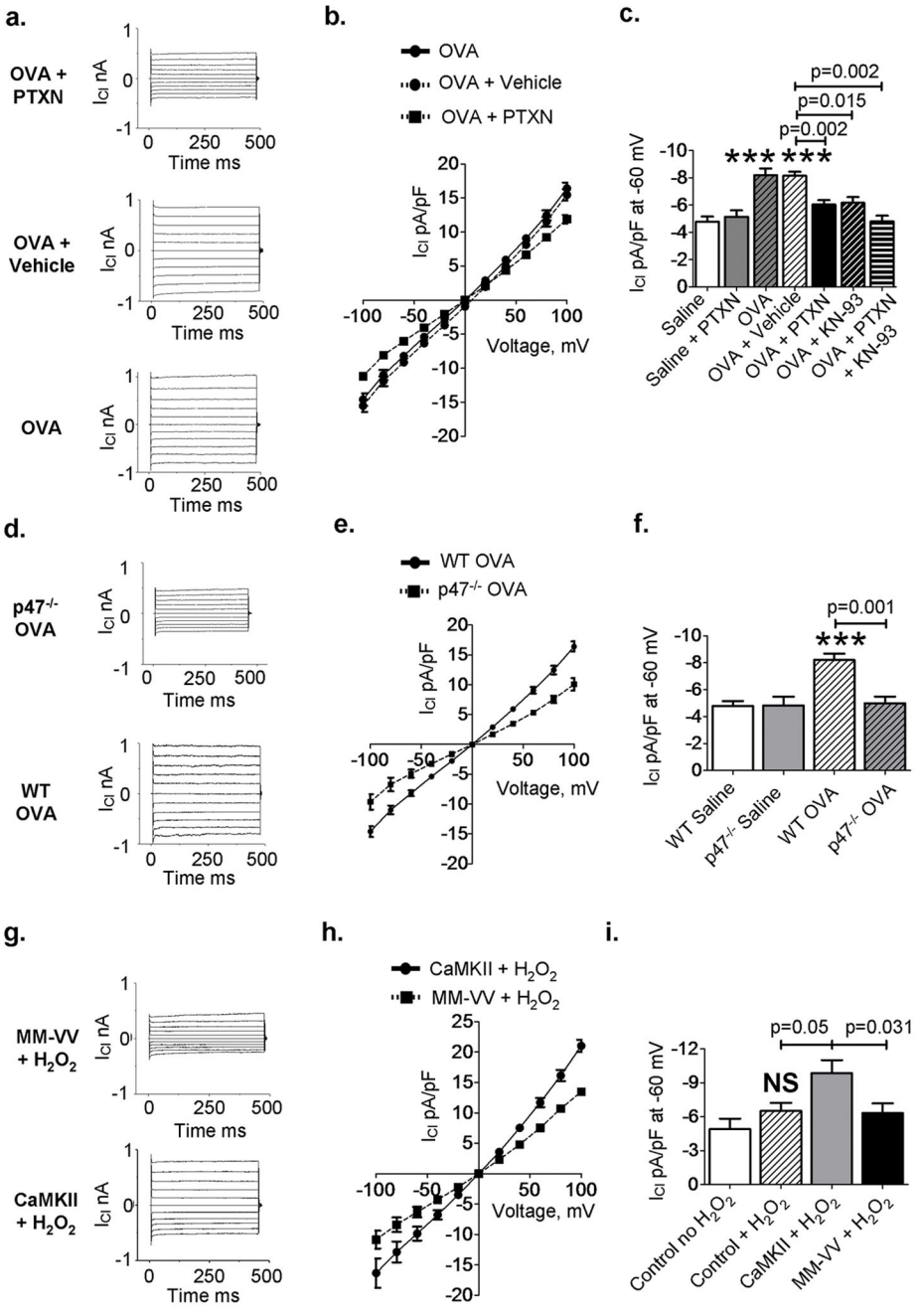

Fig. 4. Ox-CaMKII increases ICl in the airway epithelium

(A) Representative current traces and (B) summary current-voltage relationships from OVA WT tracheal epithelial cells untreated and treated with vehicle and PTXN. (C) Summary data for peak I_{Cl} recorded at −60 mV, a command voltage representative of respiratory epithelial cells' resting membrane potential, from tracheal epithelial cells isolated from WT OVA or vehicle-treated mice ex vivo with PTXN or PTXN and KN-93 (n > 4). (D to F) ICl in tracheal epithelial cells isolated from OVA p47$^{-/-}$ mice compared to OVA WT mice (n > 6). (G and H) I_{Cl} was measured after challenge with H_2O_2 (200 μM) in murine primary tracheal epithelial cells infected with control lentivirus or lentivirus encoding WT CaMKII

or oxidant-resistant CaMKII (MM-VV). (I) Summary data for peak I_{Cl} ($n > 5$). ***$P < 0.001$, versus controls. ANOVA with Bonferroni's correction was used to compare saline to OVA; Mann-Whitney was used for OVA-to-OVA comparison.

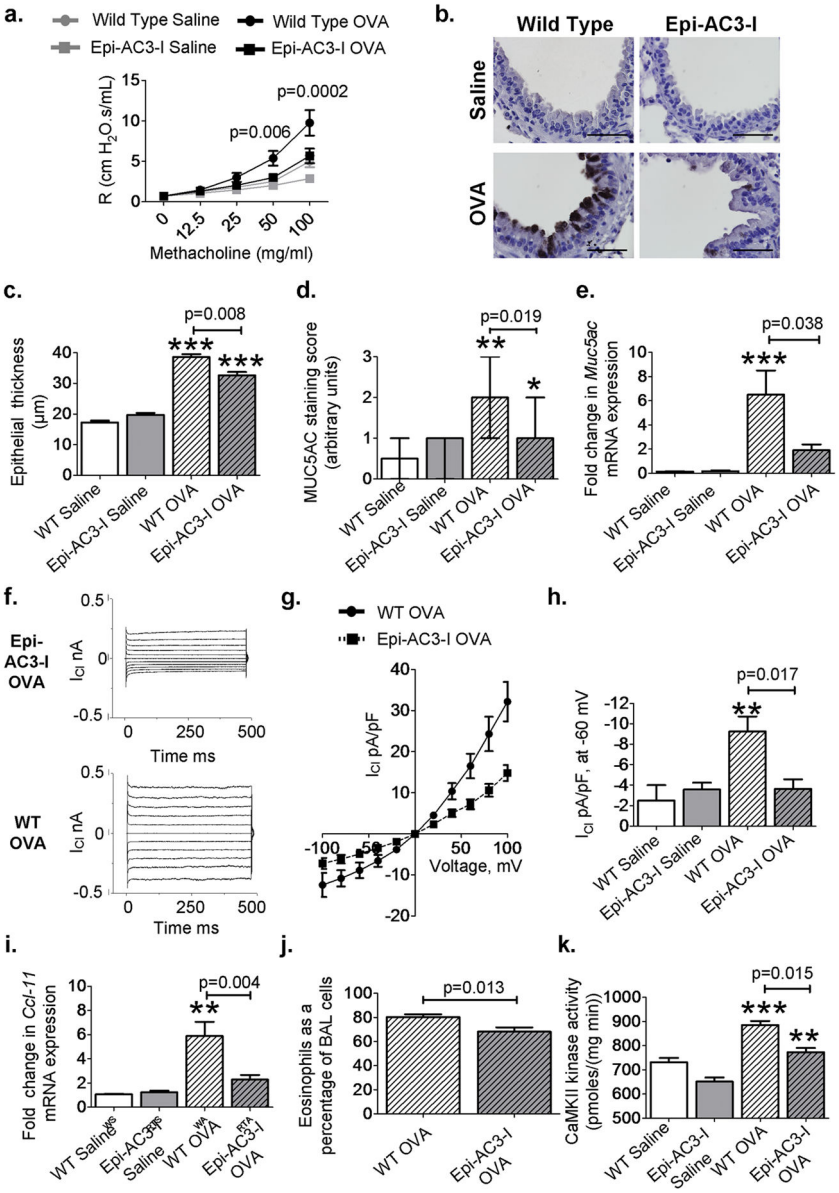

Fig. 5. Epithelial-targeted CaMKII inhibition reduces disease severity

(A) Airway resistance (R) in saline (n = 4) OVA Epi-AC3-I mice and OVA WT mice after methacholine inhalation (n > 8 per OVA group). (B) Representative images of MUC5AC-stained (brown) sections show goblet cell hyperplasia in saline and OVA WT and Epi-AC3-I lungs (×1000). (C and D) Epithelial thickness and goblet cell hyperplasia as assessed by MUC5AC staining score in saline (n = 5 per group) and OVA (n = 7 per group) airways. (E) *Muc5ac* mRNA expression in whole-lung homogenates from saline (n = 6), OVA (n = 10), and Epi-AC3-I OVA (n = 10). (F) Representative I_{Cl} current traces and (G) current-voltage relationship recorded from WT OVA and epi-AC3-I OVA respiratory epithelial cells. (H) Summary data for peak I_{Cl} recorded from tracheal epithelial cells freshly isolated from challenged mice, saline (n = 7 per group), OVA epi-AC3-I, and OVA WT mice (n = 7 per group). (I and J) *Ccl-11* mRNA (saline n = 4, OVA n = 7 per group) and BAL eosinophils (n

> 11 per group) as a percentage of total cells. (K) CaMKII activity in saline controls (n = 6), WT OVA (n = 5), and Epi-AC3-I (n = 4) mice. *P < 0.05, **P < 0.01, ***P < 0.001, versus saline control. Scale bars, 50 μm. ANOVA with Bonferroni's correction was used to compare saline to OVA; Mann-Whitney was used for OVA-to-OVA comparison.

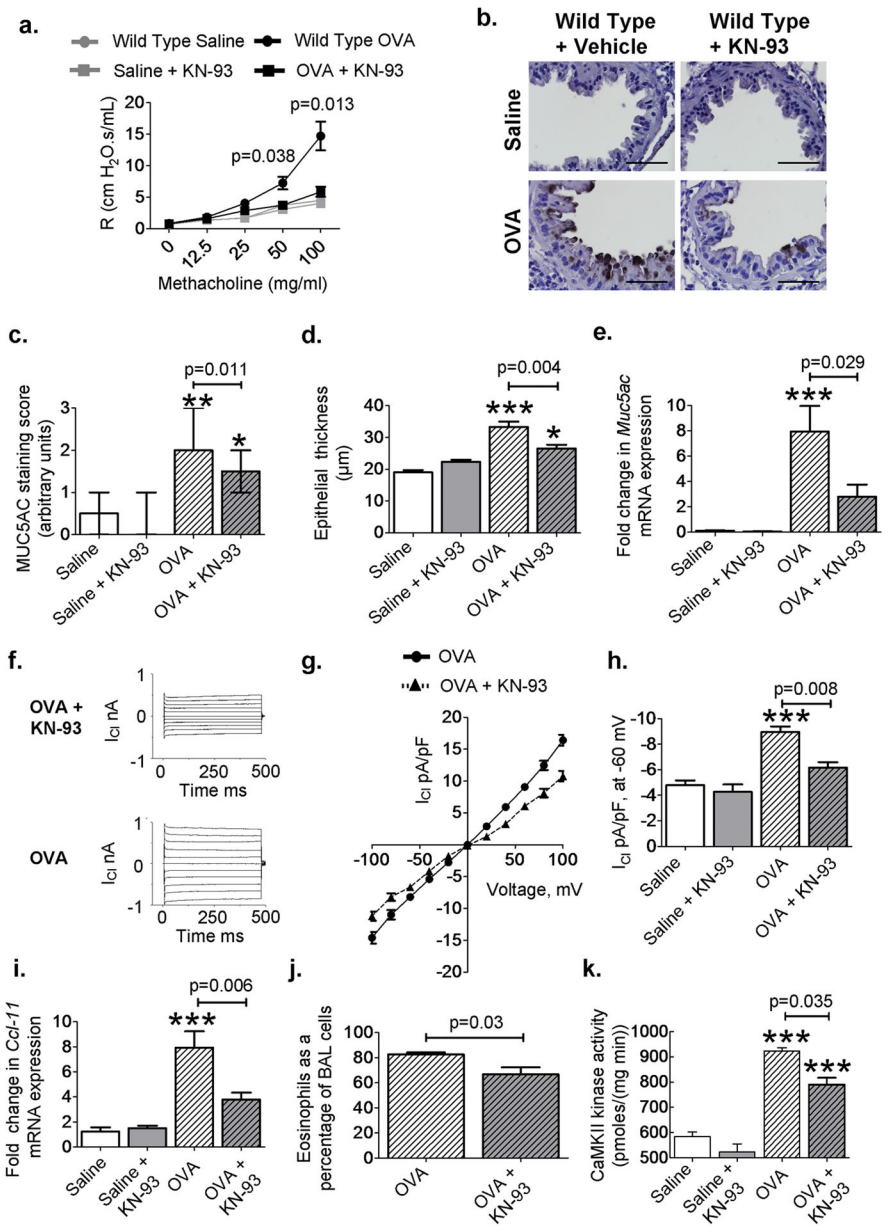

Fig. 6. Inhalation of KN-93 reduces disease severity

(A) Airway resistance (R) in mice after methacholine challenge (saline n = 5, OVA n > 7 per group). (B) Representative images of MUC5AC-stained (brown) sections showing mucin-positive cells from saline and OVA mice with or without inhaled KN-93 (×1000). (C and D) Quantification of MUC5AC staining and measurement of bronchial epithelial thickness in saline (n = 4 per group), OVA (n = 7), and OVA + KN-93 (n = 6) airways. (E) *Muc5ac* mRNA expression in saline (n = 4), OVA (n = 7), and OVA + KN-93 (n = 10). (F) Representative current traces and (G) current-voltage relationship recorded from tracheal epithelial cells isolated from WT OVA mice treated with or without KN-93. (H) Summary data for peak I_{Cl} recorded from tracheal epithelial cells freshly isolated from saline (n = 7), OVA WT (n = 10), and OVA + KN-93 (n = 4). (I and J) *Ccl-11* mRNA (saline n > 5, WT

OVAn = 8, OVA + KN-93 n = 10) and BAL eosinophils as a percentage of total cells in OVA WT mice treated with KN-93 (n = 10) compared to OVA WT mice (n = 8). (K) CaMKII activity in KN-93–treated mice (saline n > 5, WT OVA n = 3, KN-93 OVA n = 5). *P < 0.05, **P < 0.01, ***P < 0.001, versus saline control. Scale bars, 50 μm. ANOVA with Bonferroni's correction was used to compare saline to OVA; Mann-Whitney was used for OVA-to-OVA comparison.